Study of large-N Yang-Mills theory in $2+1$ dimensions

Simon Dalley
Centre for Mathematical Sciences, Cambridge University, Wilberforce Road, Cambridge CB3 0WA, England

Brett van de Sande
Geneva College, 3200 College Avenue, Beaver Falls, Pennsylvania 15010

(Received 21 October 2000; published 28 February 2001)

The bound state problem in $(2+1)$-dimensional large-N Yang-Mills theory is accurately solved using the light-front Hamiltonian of transverse lattice gauge theory. We conduct a thorough investigation of the space of couplings on coarse lattices, finding a single renormalized trajectory on which Poincaré symmetries are enhanced in bound state solutions. Augmented by existing data from finite-N Euclidean lattice simulations, we obtain accurate estimates of the low-lying glueball spectrum at $N=\infty$.

DOI: 10.1103/PhysRevD.63.076004 PACS number(s): 11.15.Tk, 11.10.Jj, 12.38.Bx, 13.85.Ni

I. INTRODUCTION

Yang-Mills theories are theoretically interesting in $2+1$ dimensions because their properties are very similar to the corresponding theory in $3+1$ dimensions, yet they can be handled much more accurately; see Ref. [1] for a review of properties and extensive references. They appear to exhibit linear confinement of heavy sources, a discrete spectrum of (glueball) bound states, and a finite-temperature transition. Teper has recently performed a comprehensive analysis, using the standard tools of Euclidean $SU(N)$ lattice gauge theory, of $(2+1)$-dimensional Yang-Mills theories at $N=2$, 3, 4, and 5. Hamiltonian lattice calculations have also recently been performed for finite N [2,3] and, though less comprehensive, the results are mainly consistent. With data at enough values of N, one can contemplate an extrapolation to $N=\infty$. This is a limit of special interest for ''analytic'' approaches to gauge theory, which often take advantage of large-N simplifications. In the absence of any other criteria for the errors involved, the only way to know how well ''analytic'' approaches are doing, for example those of Refs. [4,5], is to compare with lattice data and their extrapolation to large N.

A related question is: how close is $N=\infty$ to small N? This question can only be faithfully answered once there are accurate results in both limits. The $1/N$ expansion [6] is typically an asymptotic one and, *a priori*, observables in the two limits need not be close in value. The existing finite-N data suggest strong suppression of corrections to the large-N limit [1,7], a conclusion that was speculated about much earlier [8], on the basis of less reliable lattice data. If true, this fact deserves a deeper understanding.

The main objective of this paper is to address these issues for $(2+1)$-dimensional Yang-Mills theory with explicit calculations at $N=\infty$. In Refs. [10,11] (see also [14]) we used the large-N limit of $(2+1)$-dimensional Yang-Mills as a test for developing the transverse lattice method of solving non-Abelian gauge theories [12]. Based on an improved understanding of the sources of error in that calculation, we perform here a calculation at the next level of approximation. We obtain a renormalized light-front Hamiltonian on the transverse lattice for both the pure-glue and heavy-source sector. From this, we obtain the glueball spectrum and the heavy-source potential. Existing finite-N data, combined with our explicit large-N results, are used to determined the first few coefficients of the $1/N^2$ expansion of glueball masses in string tension units.

In the next section we briefly review the transverse lattice method, the details of which have been covered elsewhere [10,11,13]. Section III describes the numerical search for the renormalized Hamiltonian via tests of Poincaré invariance. Our thorough investigation yields a single, well-defined candidate for the renormalized trajectory in coupling space. Results for the low-lying glueball eigenstates on this trajectory and the first few coefficients of the $1/N^2$ expansion of their masses are given. This improves upon current estimates of the large-N limit, allowing us to accurately verify that corrections to it are highly suppressed.

II. TRANSVERSE LATTICE IN $2+1$ DIMENSIONS

Adapted to $2+1$ Yang-Mills theory, the Bardeen-Pearson transverse lattice gauge theory consists of continuum gauge potentials $\{A_0,A_2\}$ and space-time co-ordinates $\{x^0,x^2\}$, together with gauge-covariant transverse link variables $M(x^1)$ running between sites at x^1 and x^1+a on a transverse lattice of spacing a. We also use the light-front combinations $x^\pm=(x^0\pm x^2)/\sqrt{2}$, $A^\pm=(A^0\pm A^2)/\sqrt{2}$, etc. Discrete light cone quantization (DLCQ) [15] and Tamm-Dancoff cutoffs on the number of partons are used as intermediate regulators. These are extrapolated following the analysis of Ref. [11]. DLCQ means that we impose anti-periodic boundary conditions $x^-\sim x^-+2\pi K/P^+$, where P^+ is the total light-front momentum, and K is an integer cutoff. x^+ remains continuous and infinite, and is used as a canonical time variable to derive a light-front Hamiltonian P^-. The most general action, from which P^- will be derived canonically, must allow all gauge invariant operators that respect the Poincaré symmetries unviolated by the (gauge invariant) cutoffs. Since we will explicitly extrapolate the DLCQ and Tamm-Dancoff cutoffs, only local dimension 2 operators with respect to $\{x^+,x^-\}$ co-ordinates will be included at the outset. In the discussion hereafter we assume this limit has be taken.

Near the transverse continuum limit $a\to 0$ corresponding

to $SU(N)$ Yang-Mills, one expects M to take values in $SU(N)$. However, away from this limit one can allow M to be a general $N\times N$ complex matrix, provided it still gauge transforms covariantly. One must then search this larger class of lattice theories for the renormalized trajectory that leads one to the continuum limit $SU(N)$ Yang-Mills theory. Physical results are invariant along this trajectory and equal to the values in the full continuum limit. The trajectory may be found by renormalization group transformations in the neighborhood of a fixed point (continuum limit). However, this is difficult for the present formulation. There are (roughly) two possibilities for the behavior of M at a given point in the space of couplings constants: M is a massive degree of freedom ($M=0$ is the classical minimum); or, the ''radial'' part of M condenses. We expect the latter to be the case near the $a=0$ limit of Yang-Mills, where the action should be minimized near values of M in $SU(N)$ rather than $M=0$. Dealing with the condensation of the radial part, or using unitary matrices for M from the outset [9], is tricky in light-front quantization. This is what makes an analysis near $a=0$ difficult. On the other hand, it is straightforward to perform canonical light-front quantization about $M=0$, when this is a stable minimum. If the renormalized trajectory passes into such a region, we can then study it.

An alternative way to find the renormalized trajectory is to use symmetry [16]. Generally speaking, we can define a quantum field theory by symmetry—in our case gauge and Poincaré invariance—and a particular continuum limit (there may be more than one). There is actually no reason why we cannot take a partial continuum limit, a limit in some space-time directions but not in others, since Poincaré invariance should relate them. Thus, in Ref. [11] we proposed to take the continuum limit of Yang-Mills theory in the $\{x^0,x^2\}$ directions, and tune couplings to impose full Poincaré invariance at finite transverse cutoff a. This procedure can be carried out using light-front quantization about $M=0$. Although this regime apparently cannot contain the Poincaré-invariant theory at $a=0$, numerical evidence for the existence of a renormalized trajectory was given, and has been extended to $3+1$ Yang-Mills theory [13]. In this paper, we present conclusive numerical evidence for the case of $2+1$ Yang-Mills theory.

For practical calculations, the remaining allowed operators in the action must be pared down to a finite number of independent parameters, and one must find some reasonable criteria to test Poincaré invariance. We now develop these necessary approximations, following closely our previous work.

A. Pure-glue sector

To reduce the space of couplings to a finite dimension, we use various approximations:

(1) quadratic canonical momentum operator P^+,
(2) light-front momentum-independent couplings,
(3) transverse locality, and
(4) expansion in gauge-invariant powers of M.

The reasoning behind them is described in more detail in Ref. [13]. We only note here, that a poor choice of approximation will simply mean that we cannot get close to the renormalized trajectory, if it exists, and accuracy will suffer accordingly. The principle physical approximation, item (4) is the ''color-dielectric'' expansion about $M=0$, which is applied to the light-cone gauge-fixed Hamiltonian rather than the action.

We have studied the light-cone Hamiltonian derived from the following $SU(N)$ gauge-invariant action in the large-N limit

$$A=\int dx^0dx^2\sum_{x^1}\overline{D}_\alpha M(x^1)(\overline{D}^\alpha M(x^1))^\dagger - V_{x^1} - \frac{1}{2G^2}\mathrm{Tr}\{F^{\alpha\beta}F_{\alpha\beta}\} \tag{2.1}$$

where $\alpha\in\{0,2\}$ and

$$\overline{D}_\alpha M(x^1)=(\partial_\alpha+iA_\alpha(x^1))M(x^1)-iM(x^1)A_\alpha(x^1+a) \tag{2.2}$$

is the tranvserse lattice covariant derivative. The ''potential'' term is

$$\begin{aligned}V_{x^1}=&\mu^2\mathrm{Tr}\{M(x^1)M^\dagger(x^1)\}\\&+\frac{\lambda_1}{aN}\mathrm{Tr}\{M(x^1)M^\dagger(x^1)M(x^1)M^\dagger(x^1)\}\\&+\frac{\lambda_2}{aN}\mathrm{Tr}\{M(x^1)M(x^1+a)M^\dagger(x^1+a)M^\dagger(x^1)\}\\&+\frac{\lambda_3}{aN^2}(\mathrm{Tr}\{M(x^1)M^\dagger(x^1)\})^2.\end{aligned} \tag{2.3}$$

In light-cone gauge $A_-=0$ and after eliminating A_+ by its (constraint) equation of motion, the corresponding light-front Hamiltonian is

$$\begin{aligned}P^-=&\sum_{x^1}\int dx^- -\frac{G^2}{4}\mathrm{Tr}\left\{J^+(x^1)\frac{1}{\partial_-^2}J^+(x^1)\right\}\\&+\frac{G^2}{4N}\mathrm{Tr}\,J^+(x^1)\frac{1}{\partial_-^2}\mathrm{Tr}\,J^+(x^1)+V_{x^1}\end{aligned} \tag{2.4}$$

$$\begin{aligned}J^+(x^1)=&i(M(x^1)\overleftrightarrow{\partial}_-M^\dagger(x^1)\\&+M^\dagger(x^1-a)\overleftrightarrow{\partial}_-M(x^1-a)).\end{aligned} \tag{2.5}$$

This is the most general Hamiltonian to order M^4 that obeys the other stated approximations. It can be light-front quantized and studied in a suitable Fock space at general momenta P^+ and P^1, as detailed in Ref. [11]. The eigenvalues of the exact Yang-Mills Hamiltonian yield the glueball masses M through the relativistic dispersion relation $P^-=(M^2+(P^1)^2)/2P^+$.

B. Heavy sources

We introduce heavy sources $\phi(x^+,x^-,x^1)$ on transverse sites. They are in the fundamental representation and of mass ρ. We apply the same approximations that were made in the pure-glue sector, but here we expand to order M^2 all operators containing heavy-source fields, and work at leading nontrivial order in $1/\rho$. The heavy-source action is $A_s=A+A_\phi$ where

$$A_\phi=\int dx^+dx^-\sum_{x^1}(D_\alpha\phi)^\dagger D^\alpha\phi-\rho^2\phi^\dagger\phi - \frac{\tau_1}{NG^2}\mathrm{Tr}\{F^{\alpha\beta}(x^1)F_{\alpha\beta}(x^1)W(x^1)\} - \frac{\tau_2}{NG^2}\mathrm{Tr}\{M^\dagger(x^1)F^{\alpha\beta}(x^1)M(x^1)F_{\alpha\beta}(x^1+a)\} \tag{2.6}$$

and

$$W(x^1)=(M^\dagger(x^1)M(x^1)+M(x^1)M^\dagger(x^1)). \tag{2.7}$$

$D_\alpha=\partial_\alpha+iA_\alpha(x^1)$ is the usual covariant derivative for the plane $\{x^0,x^2\}$. After gauge fixing $A_-=0$, eliminating A_+ in powers of M from its constraint equation, and discarding the higher orders in M, the Hamiltonian resulting from A_s which satisfies the approximations is

$$P_s^-=\int dx^-\sum_{x^1}\frac{G^2}{4}\mathrm{Tr}\left\{\frac{J^+_{\mathrm{tot}}}{\partial_-}\frac{J^+_{\mathrm{tot}}}{\partial_-}\right\}-\frac{G^2}{4N}\mathrm{Tr}\left\{\frac{J^+_{\mathrm{tot}}}{\partial_-}\right\}\mathrm{Tr}\left\{\frac{J^+_{\mathrm{tot}}}{\partial_-}\right\} + V_{x^1}+\rho^2\phi^\dagger\phi+\frac{\rho\tau}{aN}\phi^\dagger W\phi+\frac{2\tau_1}{N}\mathrm{Tr}\left\{\frac{J^+}{\partial_-}\frac{J^+}{\partial_-}W\right\} + \frac{2\tau_2}{N}\mathrm{Tr}\left\{\frac{J^+(x^1)}{\partial_-}M(x^1)\frac{J^+(x^1+a)}{\partial_-}M^\dagger(x^1)\right\} \tag{2.8}$$

with

$$J^+_{\mathrm{tot}}=J^++i\phi\overleftrightarrow{\partial}_-\phi^\dagger. \tag{2.9}$$

Like P^-, P_s^- can be studied in a suitable Fock space. The eigenvalues of $v^+P_s^-$, for co-moving heavy sources of velocity v^+, are the usual excitation energies associated with the heavy-source potential [14]. If two sources are separated by na in the transverse direction x^1 and by L in the longitudinal direction x^2, then a rotationally invariant string tension would imply that, for large separations,

$$v^+P_s^-\to\sigma R,\quad R=\sqrt{a^2n^2+L^2} \tag{2.10}$$

for the lowest eigenvalue. Demanding this rotational invariance, then comparing results at $n=0$ with $L=0$, allows one to determine a in a dimensionful unit (we use G^2N) independent of σ. This fixes the relative scale between x^1 and x^2, which will be needed for testing covariance. In practice it is relatively difficult to calculate the heavy source potential in the purely transverse direction. Consequently, we measure the string tension in this direction by compactifying space and calculating the winding mode spectrum.

TABLE I. The trajectory in coupling-constant space which minimizes the χ^2 test of covariance.

m	l_1	l_2	l_3	t_1	t_2	χ^2
0.044	−0.052	−0.112	680.2	−0.661	−0.691	7.02
0.089	−0.087	−0.109	396.8	−0.780	−0.811	7.85
0.134	−0.108	−0.091	3.221	−0.896	−0.876	7.56
0.180	−0.147	−0.107	4.401	−0.943	−0.927	6.55
0.226	−0.204	−0.134	178.5	−1.098	−1.167	8.02
0.2765	−0.240	−0.153	5.48	−0.989	−1.138	7.31
0.3275	−0.308	−0.157	6.01	−1.181	−1.340	8.64

C. Poincaré invariance

We test Poincaré invariance of the theory by making measurements on eigenstates of P^- and P_s^-. It turns out that a rather simple set of tests suffices to obtain an accurate estimate of the renormalized trajectory. One of the approximations made in arriving at P^- (2.4) is transverse locality. Therefore, it makes sense to expand eigenvalues at fixed momenta (P^+,P^1) in powers of transverse momentum thus

$$2P^+P^-=G^2N(\mathcal{M}_0^2+\mathcal{M}_1^2a^2(P^1)^2+\mathcal{M}_2^2a^4(P^1)^4+\cdots). \tag{2.11}$$

Note that G has dimensions of energy, and G^2N is held finite in the $N\to\infty$ limit.[1] $\mathcal{M}_0,\mathcal{M}_1,\mathcal{M}_2,\ldots$ are dimensionless numbers which we calculate when diagonalizing P^-. The simplest requirement of covariance is that

$$\mathcal{M}_1^2a^2G^2N-1=0. \tag{2.12}$$

This ensures isotropy of the speed of light. The dimensionless quantity a^2G^2N has already been determined above from the scale setting procedure via the string tension. Further conditions come from higher order corrections in P^1 in Eq. (2.11). In this work we will use only the condition (2.12) for the lowest-mass glueballs, together with conditions of rotational invariance in the heavy-source potential, to test the space of couplings of P^-. If our reasoning is correct and our approximations valid, we should find a well-defined trajectory on which the conditions (2.12) are accurately satisfied—in practice we introduce a χ^2 test to quantify this. Moving along this trajectory should correspond to changing the spacing a. Eventually this would take us to the transverse continuum limit, but we will be prevented from reaching $a=0$ by the restriction $\mu^2>0$, a necessary condition for quantization about $M=0$.

[1] $aG^2\to g^2$ as $a\to0$, but since we do not approach $a=0$ we cannot use the continuum gauge coupling g.

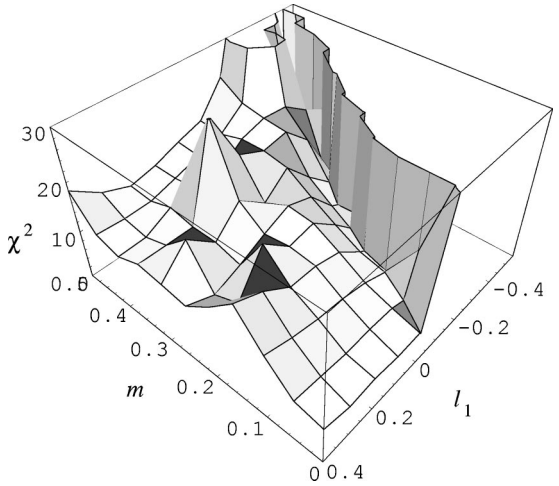

FIG. 1. Minimum χ^2 for a given m and l_1. In the blank region to the right, tachyons appear in the spectrum.

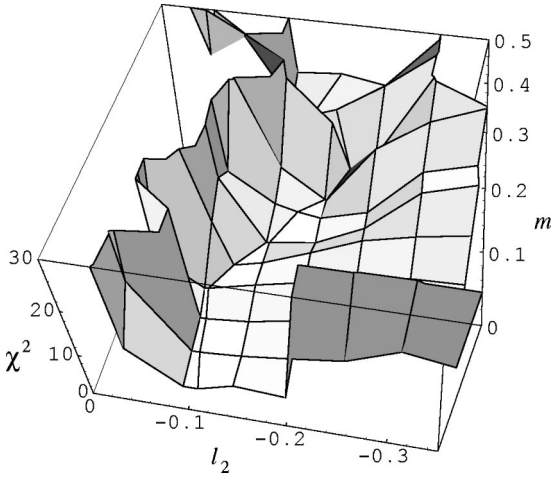

FIG. 2. Minimum χ^2 for a given m and l_2.

III. RESULTS

A. χ^2 charts

It is convenient to form dimensionless versions of the other couplings

$$m^2=\frac{\mu^2}{G^2N}, \quad l_i=\frac{\lambda_i}{aG^2N}, \quad t_i=\frac{\tau_i}{\sqrt{G^2N}}. \tag{3.1}$$

The basic technique we follow is to search this space, with the χ^2 test, for an approximation to a renormalized trajectory on which observables show enhancement of space-time symmetries violated by the cutoff a. The χ^2 test is made up of variables to test isotropy of the speed of light in dispersion of low-lying glueballs, rotational invariance of the string tension, and rotational invariance of the potential at intermediate source separations. Since we can expect to do better with some variables than others, the weights are adjusted until we produce a sharp trajectory in coupling space where χ^2 is minimized to roughly one per effective degree of freedom. In fact, altering the weights typically changes the sharpness of the trajectory and not its location. The optimum trajectory is tabulated in Table I. Full details on our computations are available at [17].

Figures 1 and 2 show χ^2 charts for a range of values of m vs l_1 and m vs l_2 near the renormalized trajectory.[2] In each case the renormalized trajectory appears at the bottom of a well-defined and unique χ^2-valley, running from large to small m. The behavior of the lattice spacing as one moves along the renormalized trajectory is shown in Fig. 3. As expected, the lattice spacing gradually decreases with m^2 but never becomes zero for $m^2>0$. The fluctuations are due mainly to the difficulty in establishing the scale $\sqrt{\sigma}$. Since the χ^2 is stable and small over a range of lattice spacings, we will use the point of smallest lattice spacing ($m=0.044$) to extract physical quantities.

B. Rotational invariance

The heavy-source potential is displayed in Fig. 4. It shows better restoration of spatial symmetry than previously obtained [11]. The potential in the continuum spatial direction x^2 is a fit to the lowest eigenvalue as a function of L of the form

$$v^+P_s^-=0.154LG^2N+0.183\sqrt{G^2N}-\frac{0.178}{L}. \tag{3.2}$$

One must be careful when interpreting Eq. (3.2) since the Coulomb potential in $2+1$ dimensions is logarithmic. The form (3.2) should be appropriate except at the very smallest L, where Coulomb corrections are expected. The $1/L$ term is a universal correction expected on the grounds of models of flux-string oscillations [18]. Universality implies that its coefficient should be invariant along the renormalized trajectory. In fact, we find that it varies slowly, a symptom that our approximation to the renormalized trajectory is not an exact scaling trajectory for this quantity and/or the form (3.2) is not sufficient to fit the potential.

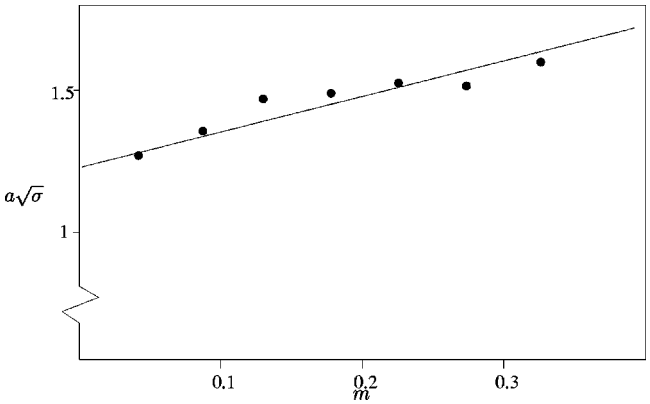

FIG. 3. Variation of the transverse lattice spacing along the Lorentz trajectory. The fit is $1.275m+1.23$.

[2]The behavior of l_3, which is always very large, is clarified in Ref. [11].

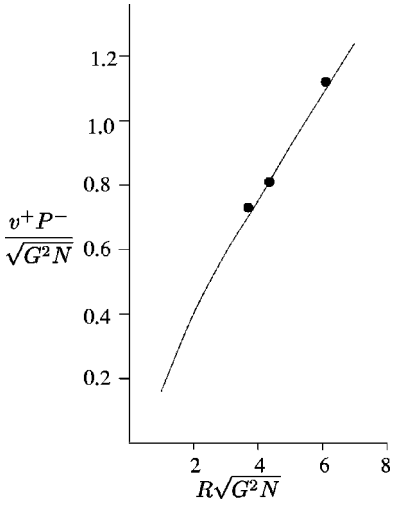

FIG. 4. The heavy-source potential. Solid line is fit to potential for sources with x^2 separation only; data points are values at one-link transverse separation and x^2 separation $L\sqrt{G^2N}=0,2.5,5$.

C. Glueballs

The spectrum of glueballs in $2+1$ dimensions can be classified by $|\mathcal{J}|^{\mathcal{PC}}$, where $\mathcal{J}$ is $SO(2)$ spin, $\mathcal{C}$ is charge conjugation, and the parity $\mathcal{P}$ is spatial reflection $x^1\rightarrow -x^1$. Combinations of $\pm\mathcal{J}$ form parity doublets if states are Lorentz covariant. On the transverse lattice, there is enough symmetry to determine $\mathcal{C}$, $\mathcal{P}$ and $|\mathcal{J}|\bmod 2$. Additionally we can examine the shape of wave functions to help distinguish the spin of states.

The lightest glueball is a 0^{++}; its mass along the renormalized trajectory is shown in Fig. 5. The anisotropy of the speed of light in the 0^{++} dispersion is less than 3% for all the low χ^2 points. For the point of smallest a, $\mathcal{M}_{0^{++}}=4.10(13)\sqrt{\sigma}$. Here, we have estimated a 2–3 % error from extrapolations in DLCQ and Tamm-Dancoff cutoffs based on known analytic behavior [11], and another 2–3 % from

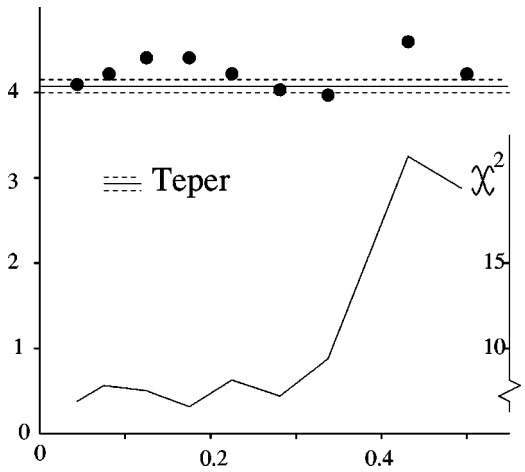

FIG. 5. The variation of the lightest glueball mass, calculated along the renormalized trajectory, is shown as data points; the associated variation of the χ^2 is also indicated. The solid horizontal line is at the value of Teper's extrapolation to $N=\infty$ of his finite-N masses (his error estimate is shown as the dotted band).

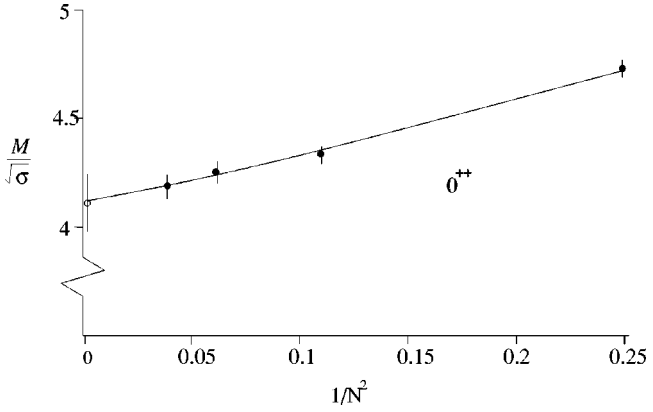

FIG. 6. Fit to lowest glueball mass as a function of N. Solid circles: Teper's finite-N data. Open circle: the large-N result from this paper.

systematic finite-a errors. The fractional finite-a error estimate is based upon deviations from the relativistic dispersion condition (2.12). Figure 5 also shows the result of Teper, $\mathcal{M}_{0^{++}}(N\rightarrow\infty)=4.065(55)\sqrt{\sigma}$, who fit his finite-$N$ data to a form $A+B/N^2$ in order to estimate the large-N limit. Teper's large-N extrapolation and our independent direct calculation are in agreement.[3]

Fitting Teper's finite-N data together with our large-N result we find

$$\frac{\mathcal{M}_{0^{++}}}{\sqrt{\sigma}}=4.118(13)+\frac{1.55(22)}{N^2}+\frac{3.38(73)}{N^4}. \qquad (3.3)$$

See Fig. 6. This gives a better estimate of the large-N limit than using one or the other data set alone.

Although we have made improvements to the calculation of σ, the dominant error in Fig. 5 still comes from the fluctuation of this quantity; in particular, the determination of σ from the longitudinal direction x^2 is a big source of error in determining the relative scales. This error becomes so severe for most heavier glueball states, which exhibit poor covariance, that an alternative method must be used for accurate results. To remove most of the error when dealing with heavier glueballs, we set $\mathcal{M}_{0^{++}}/\sqrt{\sigma}$ to the large-N value estimated in Eq. (3.3), then recalculated the renormalized trajectory with this constraint, *id est* we calculate mass ratios. To improve covariance in the lighter glueballs, at the expense of heavier states, we also restricted the χ^2 to test only the dispersion of the lowest states in each charge-conjugation sector. The resulting mass ratios, at the point of lowest χ^2 on the new renormalized trajectory, are shown in Table II. We also show the fit to the form

[3]We note that there are other finite-N lattice results which do not agree with Teper's. Recent Hamiltonian lattice calculations [3] yield $\mathcal{M}_{0^{++}}=3.88(11)\sqrt{\sigma}$ for SU(3) compared to $\mathcal{M}_{0^{++}}=4.329(41)\sqrt{\sigma}$ in Ref. [1].

TABLE II. Mass ratios for lightest glueball excited states, showing our $N=\infty$ measurement and fit coefficients including finite-N data from Ref. [1]. The 2^{-+} and 0_*^{++} states were not covariant enough for reliable error estimates, and only Teper's finite-N extrapolation is shown.

		Fit coefficients		
$\lvert\mathcal{J}\rvert^{\mathcal{P}C}$	$\mathcal{M}/\mathcal{M}_{0^{++}}$	C	B	A
0^{--}	1.35(5)	−14.58(1.47)	2.983(191)	1.349(6)
2^{++}	1.60(17)	3.233(2.724)	−1.144(856)	1.743(51)
0_*^{--}	1.82(6)	−5.839(7.488)	1.136(941)	1.824(25)
2^{-+}	1.77(?)	-	0.659(246)	1.697(57)
0_*^{++}	1.28(?)	-	0.770(399)	1.520(38)

$$\frac{\mathcal{M}}{\mathcal{M}_{0^{++}}} = A + \frac{B}{N^2} + \frac{C}{N^4} \tag{3.4}$$

including Teper's data. The convergence in $1/N^2$ is illustrated in Fig. 7.

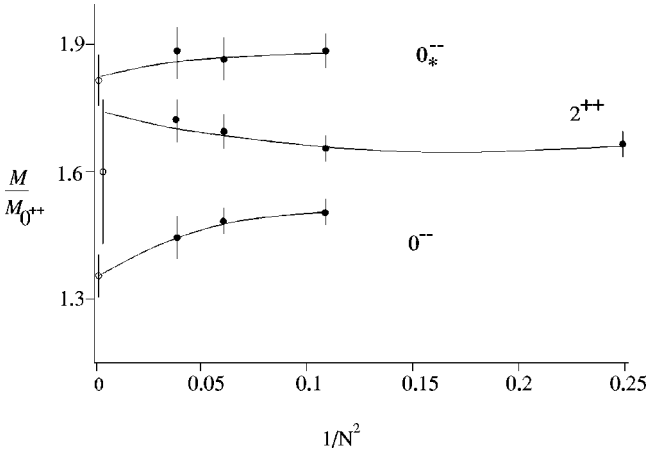

FIG. 7. Variation of excited glueball mass ratios with N. Solid circles: Teper's finite-N data. Open circles: the large-N result from this paper.

IV. CONCLUSIONS

We have found that our improved transverse lattice calculations for $2+1$ Yang-Mills theory in the large-N limit are consistent with existing finite-N data from an independent lattice method. Although both make use of lattice regulators, the methods use different quantization procedures, elementary degrees of freedom, regulators, gauge fixing, and renormalization techniques. By combining the finite-N and large-N results, we have obtained accurate estimates of the lightest glueball masses and mass ratios for any N in $2+1$ dimensions. These should provide a useful benchmark for analytic studies. We are able to confirm that $O(1/N^2)$ corrections to the large-N limit are typically small. The plots of mass versus $1/N^2$ could have had any shape, but they turn out to be almost straight and almost flat. The same result also seems to be true in $3+1$ dimensions [13], though the data is less precise there. Recalling how the quark model explains the (OZI) suppression of $1/N$ corrections in most channels [19], it would be interesting to know if constituent gluon models could provide an intuitive explanation of our finding.

ACKNOWLEDGMENTS

S.D. is supported by PPARC grant No. GR/LO3965. B.v.d.S. was supported by the Research Corporation. Computations were performed at the Ohio Supercomputer Center and at the Pittsburgh Supercomputer Center.

[1] M. Teper, Phys. Rev. D **59**, 014512 (1999).
[2] C. Hamer, M. Sheppeard, W-H. Zheng, and D. Schutte, Phys. Rev. D **54**, 2395 (1996); C. Hamer, *ibid.* **53**, 7316 (1996).
[3] Q. Z. Chen, X. Q. Luo, S. H. Guo, and X. Y. Fang, Phys. Lett. B **348**, 560 (1995); X. Q. Luo, Q. Z. Chen, S. H. Guo, X. Y. Fang, and J. Liu, Nucl. Phys. B (Proc. Suppl.) **53**, 239 (1997).
[4] D. Karabali and V. P. Nair, Phys. Lett. B **379**, 141 (1996); Nucl. Phys. **B464**, 135 (1996); Int. J. Mod. Phys. A **12**, 1161 (1997); D. Karabali, C. Kim, and V. P. Nair, Phys. Lett. B **434**, 103 (1998); Nucl. Phys. **B524**, 661 (1998).
[5] C. Csaki, H. Ooguri, Y. Oz, and J. Terning, J. High Energy Phys. **01**, 017 (1999); R. de Mello Koch, A. Jevicki, M. Mihailescu, and J. P. Nunes, Phys. Rev. D **58**, 105009 (1998); R. Brower, S. Mathur, and C-I. Tan, Nucl. Phys. **B587**, 249 (2000).
[6] G. 't Hooft, Nucl. Phys. **B72**, 461 (1974).
[7] M. Teper, Phys. Lett. B **397**, 223 (1997); **311**, 223 (1993); **289**, 115 (1992).
[8] S. A. Chin and M. Karliner, Phys. Rev. Lett. **58**, 1803 (1987).
[9] P. A. Griffin, Nucl. Phys. **B139**, 270 (1992).
[10] S. Dalley and B. van de Sande, Nucl. Phys. B (Proc. Suppl.) **53**, 827 (1997); Phys. Rev. D **56**, 7917 (1997).
[11] S. Dalley and B. van de Sande, Phys. Rev. D **59**, 065008 (1999).
[12] W. A. Bardeen and R. B. Pearson, Phys. Rev. D **14**, 547 (1976); W. A. Bardeen, R. B. Pearson, and E. Rabinovici, *ibid.* **21**, 1037 (1980).
[13] S. Dalley and B. van de Sande, Phys. Rev. Lett. **82**, 1088 (1999); Phys. Rev. D **62**, 014507 (2000).
[14] M. Burkardt and B. Klindworth, Phys. Rev. D **55**, 1001 (1997).
[15] H.-C. Pauli and S. J. Brodsky, Phys. Rev. D **32**, 1993 (1985); **32**, 2001 (1985).
[16] R. J. Perry and K. G. Wilson, Nucl. Phys. **B403**, 587 (1993).
[17] http://www.geneva.edu/~bvds/dave/
[18] M. Luscher, Nucl. Phys. **B180**, 317 (1981).
[19] P. Geiger and N. Isgur, Phys. Rev. D **44**, 799 (1991); Phys. Rev. Lett. **67**, 1066 (1991); Phys. Rev. D **47**, 5050 (1993).